Pergamon

Cement and Concrete Research, Vol. 27, No. 4, pp. 601–617, 1997

0008-8846/97 $17.00 + .00

PII S0008-8846(97)00027-6

REPAIR MATERIAL PROPERTIES FOR EFFECTIVE STRUCTURAL APPLICATION

P.S. Mangat* and M.C. Limbachiya**
* School of Construction, Sheffield Hallam University,
Sheffield, S1 1WB, England, UK
**Concrete Technology Unit,
Department of Civil Engineering, University of Dundee,
Dundee, DD1 4HN, Scotland, UK

(Refereed)
(Received October 8, 1996; in final form February 4, 1997)

ABSTRACT

Strength and engineering properties of three generic repair materials which are likely to influence long-term performance of repaired concrete structures were studied. Measured properties include strength, stiffness, shrinkage and creep deformations, together with the complete compressive stress-strain characteristics including post-cracking behaviour. The repair materials considered in this investigation are commercially available and widely used. These included a high performance non-shrinkable concrete, a mineral based cementitious material with no additives or coarse aggregate size particles, and a cementitious mortar containing styrene acrylic copolymer with fibre additives. Performance comparisons are also made between these materials and plain concrete mixes of similar strength and stiffness, suitable for repair applications. The results show that shrinkage of the repair materials was significantly greater than the shrinkage of normal concrete. Moreover, the shrinkage of those modified with a polymer admixture was found to be very sensitive to the relative humidity of the exposure compared to normal concrete. The post-peak strain capacity of the material modified with a polymer admixture was markedly improved leading to a more pronounced falling branch of stress-strain curve. The ultimate stress level (at a maximum load) of specially formulated repair materials varies significantly, the lowest ultimate stress being recorded for the porous mineral-based material. The inclusion of aggregates improves the mechanical properties and dimensional stability of repair materials. © *1997 Elsevier Science Ltd.*

Introduction

The durability of a material or structure refers to its ability to withstand the environmental conditions to which it is exposed. Although concrete structures have mostly performed satisfactorily during their service life, there are nevertheless significant problems which occur in many structures and the causes are often related to durability of the composite material. As a result, in recent years, repair, refurbishment and maintenance of concrete structures have

become a significant part of the total cost of construction worldwide [1]. Different repair methods and generic materials are currently used to overcome damage in deteriorated structures. The basic mechanical and physical interactions of such available products and the substrate on which they are used need to be established before assessment can be made and suitable repair materials chosen. Under current practice, there are no standard procedures for the design of patch repairs. Design is usually based on the experience of specialist contractors and when selection of repair materials is made, emphasis is normally given to their relative short-term properties such as strength, bond and early age plastic shrinkage/expansion etc. Although these properties indicate the immediate performance of the repair, they give little information on its long-term performance with respect to cracking and efficient composite action with the substrate materials to carry loads and deformations. Several researchers [2-6] have highlighted the potential importance of property mismatches between patch repair and reinforced concrete substrate. Therefore, there is an important need for recognising and understanding the properties of generic repair materials, which are of significance to the subsequent structural behaviours of repaired concrete members.

Experimental Details

Materials and Mixes. Three commercially available generic repair materials which are labelled A, B and C were used in this study, together with a plain concrete mix of similar strength, which was used to provide control specimens for comparison. The repair materials A, B and C are supplied as single component systems by their manufacturer, ready for on-site mixing and use and requiring only the addition of potable water. Details of the repair materials are as follows:-

Material A is a blend of Portland cement, graded aggregates of maximum size 5mm and additives which impart controlled expansion in both the plastic and hardened state whilst minimising water demand. This high performance, non-shrinkable concrete is used for the reinstatement of concrete. The material has been formulated to comply with the requirements of the DTp specification (UK) for Highway works, Clause 1704.6 control of alkali-silica reaction. A water:powder ratio of 0.13 is recommended for use and the typical density of the fresh material is 2069 Kg/m^3.

Material B is a mineral based cementitious material with no aggregate size particles or additives. It is relatively porous to allow leaching of salts to continue from contaminated concrete after its repair. A water:powder ratio of 0.16 is recommended and the typical density of the fresh material is 1575 Kg/m^3.

Material C is a single component cementitious mortar containing, microsilica, fibre reinforcement and styrene acrylic copolymer. The thixotropic nature of the product makes trowel application easy in structural repair of voids, rendering and in reprofiling of both vertical and horizontal surfaces. The recommended water:powder ratio is 0.16 and the fresh density is 1700 Kg/m^3.

Plain concrete mix used for comparison with the repair materials had constituents of Portland Cement grade 42.5 N to BS 12, 1991 [7], fine aggregate conforming to zone M of BS 882, and coarse aggregates of 10mm maximum size. The mix proportions (by weight) were 1 : 2.24 : 3.22, with a water cement ratio of 0.56 to achieve 28 day strength of 40 N/mm^2. The cement content was 343 kg/m^3.

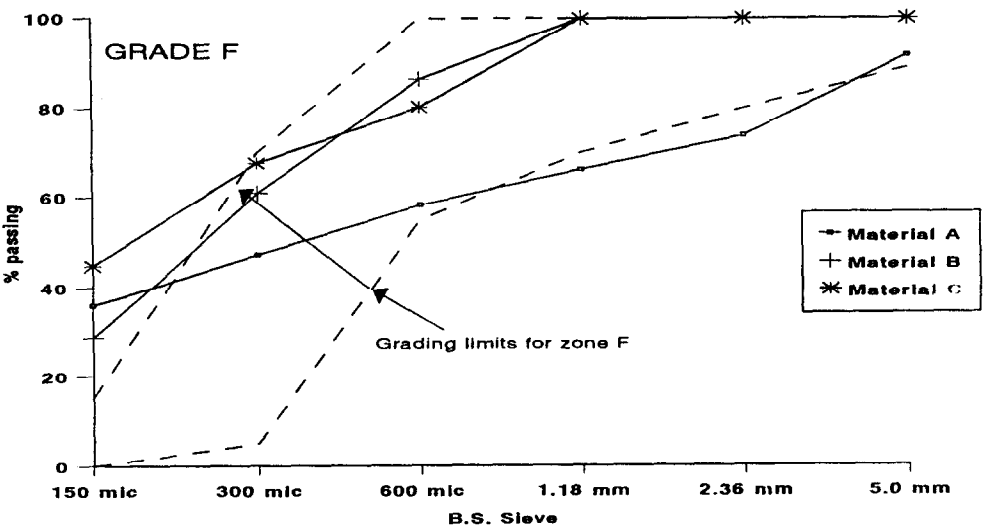

FIG. 1.
Grading curves for the repair materials.

It is apparent from the grading curves of the repair materials, Figure 1, that material A is much coarser than materials B and C. In this material, there is a significant amount of aggregates of particle size 1.18mm or greater, whereas in materials B and C, which are of similar grading, all particles sizes are much smaller than 1.18mm. In the case of the concrete mix, aggregate grading is much coarser, comprising sand of zone M and 10mm coarse aggregate.

Test Specimens, Casting and Curing

The specimens were cast in two layers on a vibrating table. The fresh material was covered with polythene sheets for 24 hours.

Strength and Elastic Modulus Tests. Compressive strength tests were performed on 100mm cubes, tested at 3, 7, 14 and 28 days, with three specimens in each case and cured in water at 20° until the test age. Also, three 100 × 100 × 500mm prism specimens were cast for each material to determine flexural strength and static modulus of elasticity at 28 days. Specimens were cured in water at 20°. All the specimens were demoulded 24 hours after casting.

Swelling and Drying Shrinkage. For each of the three repair materials and plain concrete, ten prisms of 100 x 100 x 500mm dimensions were used to measure swelling and drying shrinkage deformations. The specimens were demoulded after 24 hours and thereafter demec points, across a 200mm gauge length, were attached to the four longitudinal faces of each specimen. Subsequently, the first reading was taken and regular measurements were made thereafter. The swelling deformation of the materials was determined under total immersion in water (at 20°C) and those specimens used in the shrinkage studies were transferred to one of four different curing conditions as follows:

(a) 20°C and 30 percent R.H.
(b) 20° and 45 percent R.H.
(c) 20° and 55 percent R.H.
(d) cured in water for the first 28 days after casting, then stored in air at 20°/55% RH.

Compressive Creep. In total, four prism specimens of 100 x 100 x 500mm size were tested for each material. They were cured in water at 20° for 28 days prior to loading. Three 100mm cube specimens were also prepared to determine compressive strength at 28 days.

Compressive Stress-strain Characteristics. Prism specimens of size 75 × 75 × 300mm were prepared and cured at 20° in water. Prior to testing, elastic electrical resistance strain gauges of 30mm gauge length were attached on both longitudinal and lateral directions at the mid point on two opposite faces of the specimens in order to measure strains.

Test Procedures

The test procedures employed in this investigation are as described below.

Strength and Elastic Tests. The compressive strength tests were carried out at 3, 7, 14 and 28 days in accordance with BS 1881: part 116, 1983 [8]. The flexural strength of prism specimens was determined under four point loading in accordance with BS 1881: part 118,1983 [9], at the age of 28 days. The Young's modulus of elasticity of prism specimens was determined in accordance with BS 1881: part 121, 1983 [10].

Swelling and Drying Shrinkage. The first datum strain reading, across a 200mm gauge length, was taken at 24 hours after casting, and tests were carried out periodically thereafter for 365 days. Each shrinkage and swelling value presented in this paper is an average of strains measured across eight faces of two prism specimens. The effects of varying the curing environment on such deformation were also examined over 120 days drying period. The controlled temperature and relative humidity curing conditions were provided in a purpose built environment room.

Compressive Creep. The creep tests in this investigation were conducted in accordance with the recommendations for standard creep tests [11]. In these tests, two prisms of each material were loaded together in a standard creep rig. Each creep rig comprised steel end platens supported by nuts on four 36mm diameter tie rods of high yield steel. The axial sustained load on the specimens was applied by means of a hydraulic jack via the top platens of the rig. This load was maintained at a constant level by regular loading and tightening of the nuts against the end platens. The concentricity of the applied load was ensured by achieving reasonably similar strains on the four steel tie rods. The creep rigs were located in a temperature and humidity controlled environment set at 20° and 55% relative humidity. Two creep tests were carried out for each material at a sustained stress of 30, 45 and 55 percent of the 28 day cube strength. The initial strain on loading and subsequent increases in strain were monitored across the 200mm gauge length, on the two opposite faces of each test prism. In order to calculate the net creep strain, drying shrinkage strain was measured on separate specimens and deducted from the total strain measured on specimens in the creep rigs.

Compressive Stress-Strain Characteristics. A simple method has been developed [14] to obtain the descending portion of the stress-strain curve up to a strain of 0.007. This technique is similar to those used by other researchers [12,13]. A steel tube was made of mild steel conforming to BS 4360-43A, which was heat treated to behave elastically up to strains of 0.007. Prism specimens of repair materials were loaded in parallel with the steel tube. Tests were carried out in compressive testing machine under a constant rate of loading.

During testing, to ensure the specimen and the tube were in direct contact with the loading platen simultaneously, brass shims were used as a capping. The strain readings from the specimen and the tube were taken using two strain meters, one for the tube strain reading and the other for test specimen readings. The strain readings were recorded at regular increments of load, up to the end of test. Figure 2 shows a typical load versus the averaged recorded strains graph taken from repair material A and the steel tube in the longitudinal direction. It is clear from this figure that, after a certain applied load, both the test specimen and the tube are in complete contact with the platen and start to deform together with applied load increments. As indicated, this occurs at 375KN load in Figure 2 when the initial slopes of load-strain graphs of both repair material and the steel tube changes. From this point onwards, each further increment of loading leads to an equal increase in strain of both the test specimen and the steel tube. Hence, monitoring the steel tube strains and from the knowledge of the applied load, the specimen stress-strain behaviour can be evaluated. Volumetric strains were also calculated from this data.

Results and Discussion

Strength. Table 1 gives the results of the flexural strength and elastic modulus tests on each repair material together with the development of compressive strength. It is clear from the

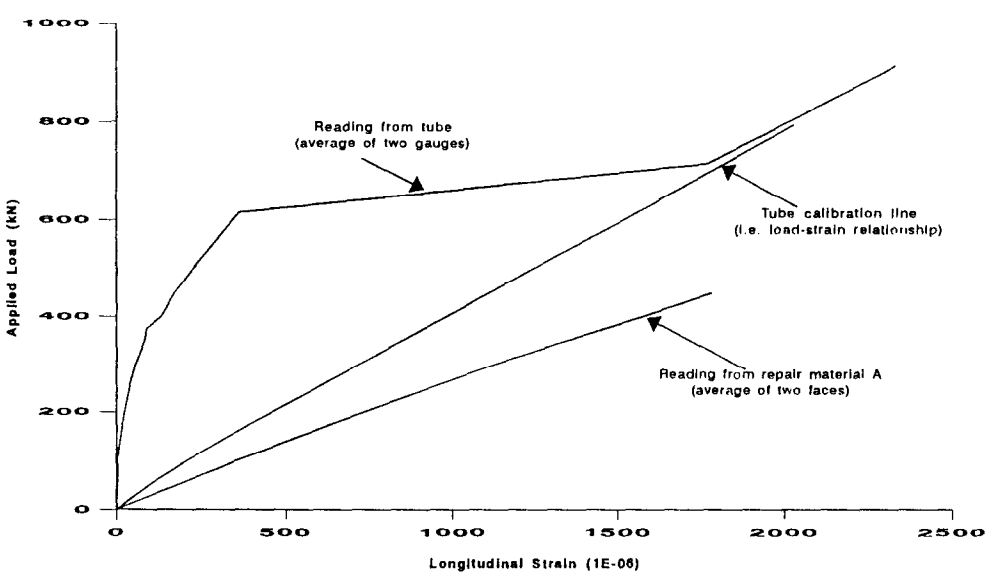

FIG. 2.
Load vs. longitudinal strain measured on test sample (material A) and steel tube.

TABLE 1

Strength Development and Elastic Modulus at 28 Days Age

Material	Compressive strength (N/mm^2) Age		Flexural Strength (N/mm^2) (at 28 days)	Elastic Modulus (kN/mm^2) (at 28 days)
A	- 3 days	36.20	7.74	31.98
	- 7 days	46.30		
	- 14 days	56.75		
	- 28 days	63.70		
B	- 3 days	25.10	4.21	19.10
	- 7 days	29.90		
	- 14 days	31.30		
	- 28 days	33.00		
C	- 3 days	31.00	3.69	18.30
	- 7 days	39.70		
	- 14 days	41.95		
	- 28 days	44.00		
Concrete	-28 days	40.60	4.40	19.00

strength results that the high-performance, 'non-shrink' repair material A develops strength rapidly. Similarly the elastic modulus and modulus of rupture of material A are much greater than other materials. Repair materials B and C and plain concrete mixes have similar elastic moduli and flexure strength.

Drying Shrinkage and Swelling. Figure 3 shows results of shrinkage (20°/55%RH) and swelling deformations of the repair materials and control concrete. In addition, the influence of relative humidity of the curing environment on shrinkage are shown in Figures 4. Comparison with the curves of plain concrete (Figure 4d) shows that all repair materials exhibit greater shrinkage. It is important to note that even special formulated repair material such as material A which is designed to be non-shrink display much higher shrinkage than plain concrete. The curve for repair material C shows very rapid shrinkage for the first three weeks followed by similar rate of shrinkage as the other repair materials.

The results plotted in Figures 3 and 4 show that the styrene acrylic latex modified repair material C has much higher values of shrinkage and swelling compared to other materials. Similar results were found by Emberson and Mays [6] for SBR and vinyl acetate polymer modified cementitious material, when specimens of size 40 × 40 × 160mm were stored in a

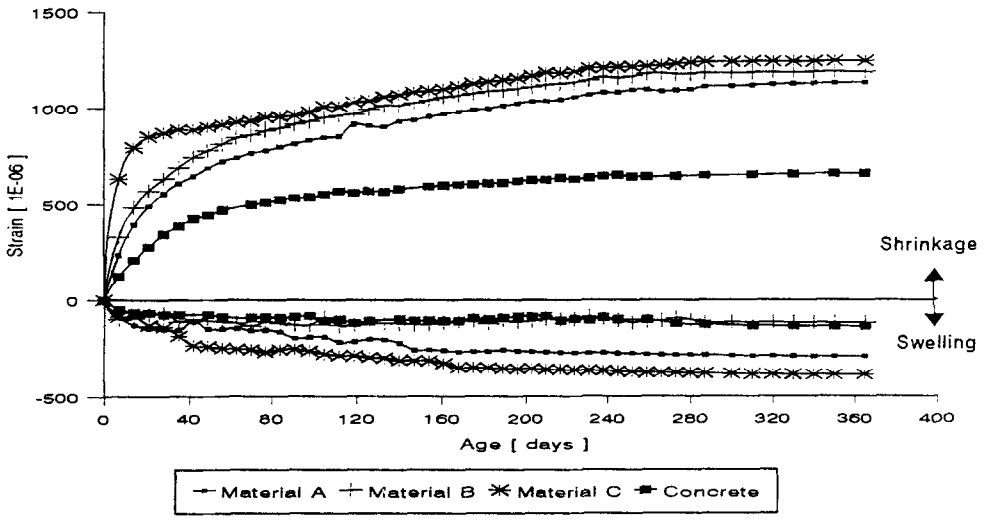

FIG. 3.
Deformation of repair materials; shrinkage at 20°C, 55% RH and swelling at 20°C, 100% RH.

control room in which the temperature varied from 12 to 22° and the relative humidity varied from 55% to 95%.

The 90 days result for shrinkage (under different conditions) and swelling deformation is given in Table 2. The large magnitude of shrinkage and swelling strains of the repair materials (especially material C) relative to plain concrete is clearly evident. Figure 4 shows that the shrinkage of specimens cured in water first for 28 days, then stored in air at 20°, 55% relative humidity is lower than specimens continuously cured at 20°, 55% R.H. after demoulding (24 hours after casting). This difference is much higher in all repair materials compared with plain concrete. Also, the increase in shrinkage under curing at 30% R.H. compared with 55% R.H. curing is much greater in this material compared with plain concrete. Therefore, the risk of shrinkage cracking with the use of these repair materials in practical situations is greater.

Compressive Creep. Some typical creep curves of the four materials at stress/strength ratios of 0.30, 0.45 and 0.55 are plotted in Figure 5, showing an instantaneous elastic strain upon loading and the rate at which creep strains increase with time. All creep strains are an average of four specimens. The shapes of the curves for each material are similar, thus indicating that the creep phenomenon in each case is basically the same. The instantaneous elastic strains and the 90 day creep strain are given in Table 3. Repair material C shows the greatest creep strains (e.g. 1871, 2552, 3137 microstrain at stress/strength ratios of 0.30, 0.45 and 0.55 respectively) due to the addition of latex modifiers in its preparation. Similar evidence of high creep strain for vinyl acetate polymer modified cementitious material is given by data from Emberson and Mays [6]. While the creep strains of materials A and B is quite similar or greater (at 55% stress/strength ratio) than that of concrete.

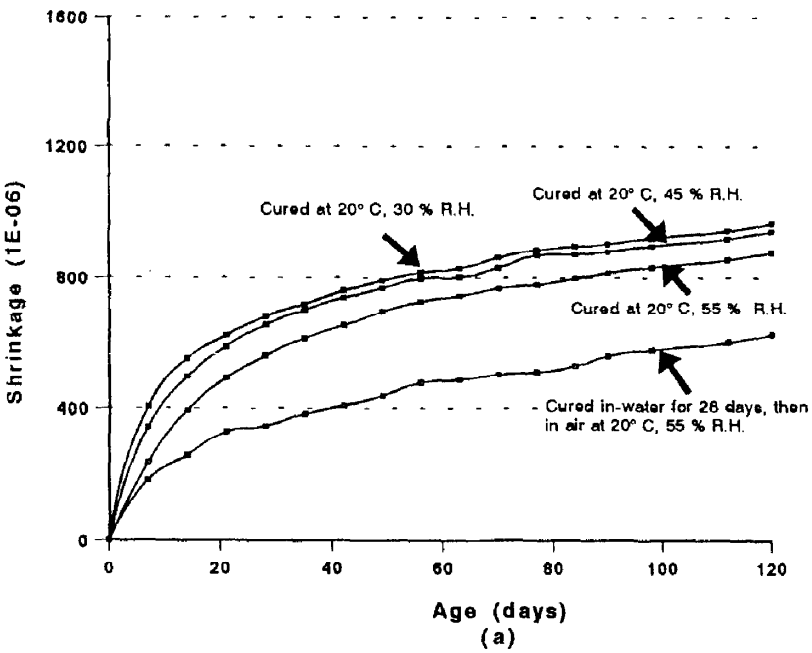

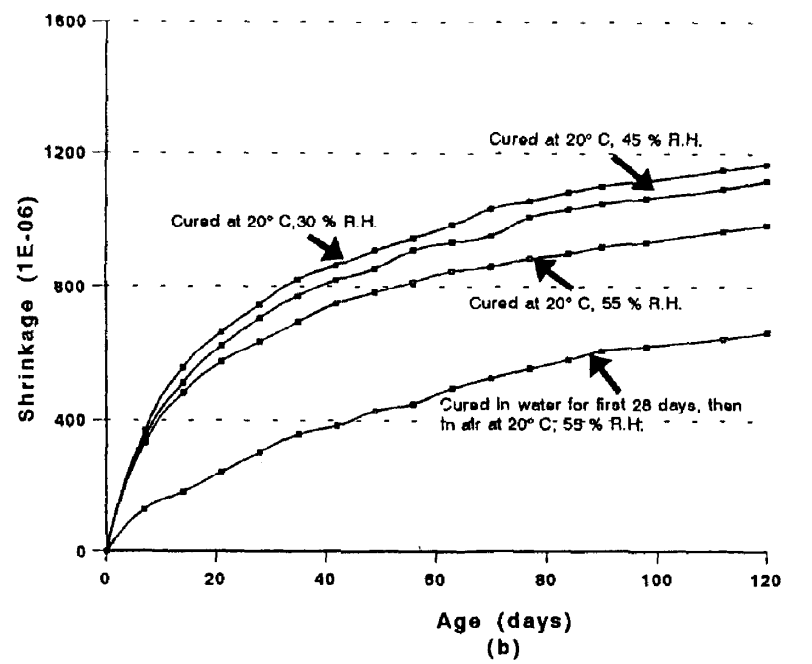

FIG. 4.
Influence of relative humidity (at 24 hours after casting) on shrinkage of (a) Material A; (b) Material B; (c)Material C and (d) Concrete.

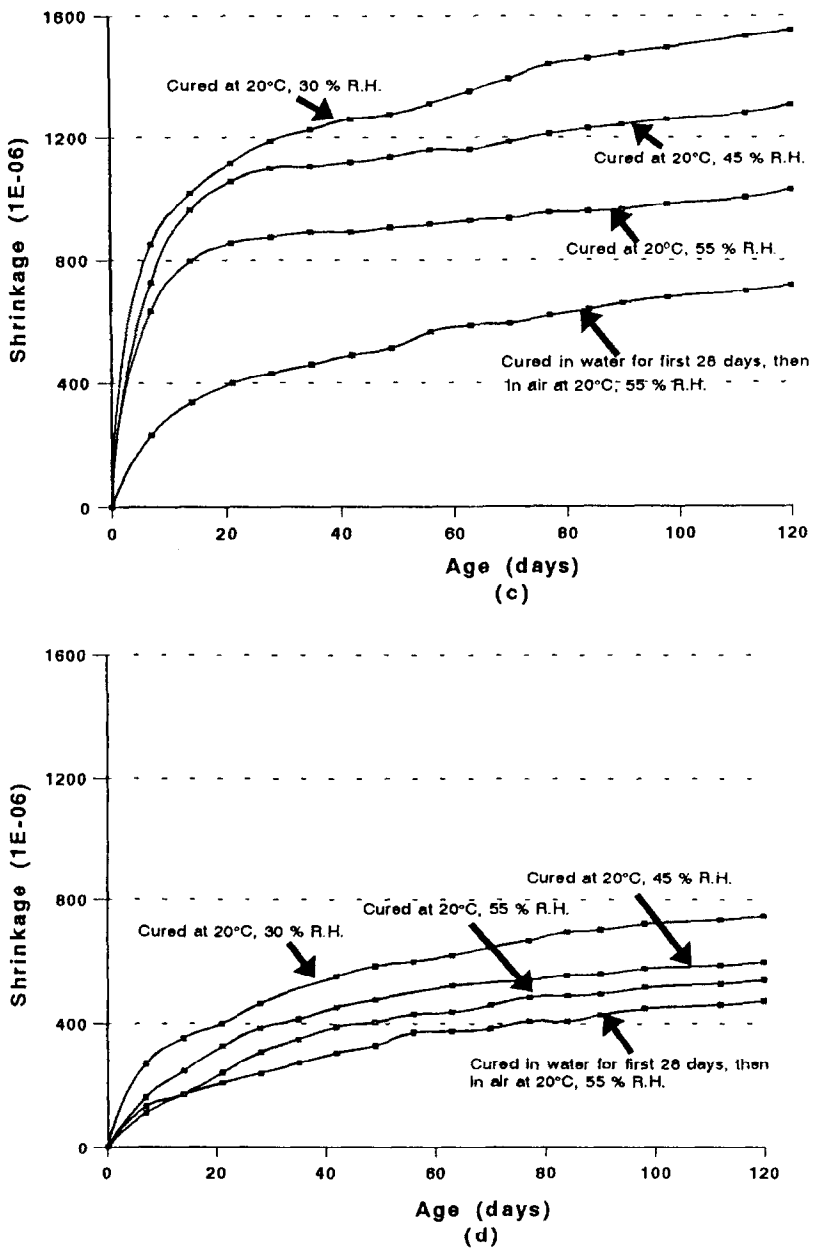

FIG. 4. *Continued*

Compressive Stress-Strain Behaviour. Typical stress-strain curves of the repair materials and plain concrete are plotted in Figure 6, showing the longitudinal, lateral and volumetric strain. Also, the experimental results for generic repair materials and concrete are recorded in Table 4, which include strain capacity (longitudinal, lateral and volumetric) at initiation stress and critical stress. One of the most interesting aspects of these tests was the similarity in the

TABLE 2

Shrinkage and Swelling Deformation Strains at 120 Days (Microstrain)

Repair materials	Shrinkage at 20°C and relative humidity of; 55%	45%	30%	Swelling (at 20°C and 100% R.H.)
A	879	945	970	214
B	984	1115	1165	138
C	1028	1308	1551	287
Concrete	541	600	747	119

ascending portion between the repair materials and concrete specimens, while the descending portions of some repair material were very different. The existence of the descending branch means that the material has a capacity to withstand some load after the maximum load has been passed because the linking of microcracks is delayed before a complete breakdown. From the Figure 6, in high strength repair material A both ascending and descending parts of the curve are steeper compared to other two repairs (B and C) and this implies a more brittle type of behaviour.

Initiation stress. The boundary between stable crack initiation and propagation zones is referred to as the crack "initiation stress." This crack initiation stress corresponds to the point when poisson's ratio of the material starts to increase and the volumetric strain curve deviates from linearity [14,15]. Figure 7 shows the relationship between poisson's ratio and applied stress-strength ratio for the plain concrete and three different repair material specimens. The initiation stress-strength ratio for repair material C is 0.28 compared to 0.55 for the plain concrete specimens. The cause of this reduction is most-likely to be the greater interfacial surface area between the matrix and inclusions, which is generated due to polymer and fibre additions.

Critical stress. The "critical stress" has been defined as the boundary between the stable and unstable crack propagation zones [2] and this stress level is reflected by the dilation of the matrix structure. This level corresponds to the point on the stress-strain curve where a reversal of volumetric strain occurs. The critical stresses of the specimens investigated in this study were determined from the stress-strain curves and are reported in Table 4. It is clear that the range of critical stress-strength ratios is between 0.78 and 0.83 for the materials considered in this investigation.

Ultimate strain. It is clear from Figure 6 that the ultimate stress level and the post yield characteristics are influenced by the material constituents. For example, material A which has high strength and subsequent high stiffness shows the highest ultimate stress level. The ultimate strains (at maximum stress) of concrete and repair material specimens tested varied between 1300 to 6100 microstrain.

Strain capacity. The ductility of a repair patch is its ability to sustain significant inelastic deformation without any considerable variation in load resisting capacity prior to failure.

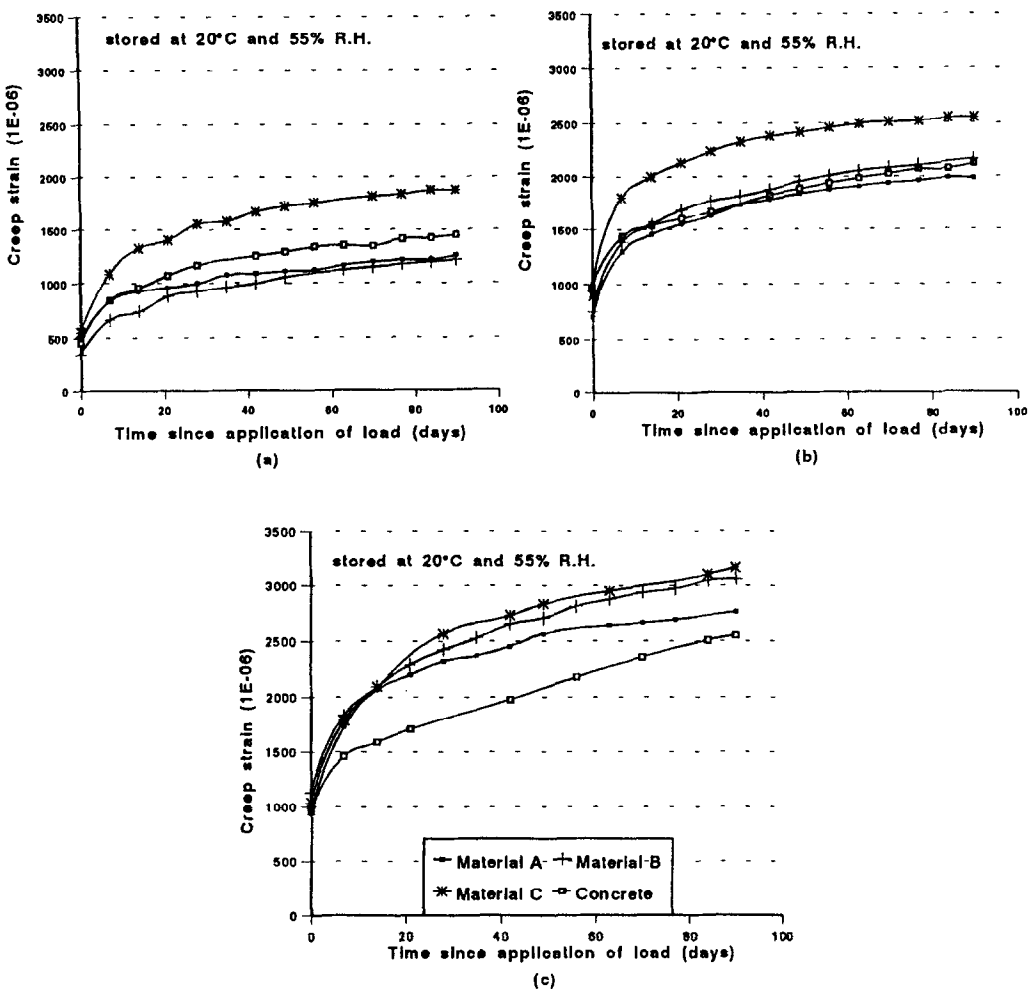

FIG. 5.
Compressive creep at (a) 30%, (b) 45% and (c) 55% stress/strength ratio.

Ductility can be measured by the toughness and strain capacity of the material at post-peak level. In the present study, the post yield strain capacity of repair materials and concrete is assessed by considering the longitudinal strain at a stress-strength ratio of 0.4 on the falling branch of the stress-strain curves in Figure 6. Figure 8 represents longitudinal strain at a post-peak stress/strength ratio of 0.4 for repair materials and plain concrete considered in this investigation. It can be seen from Figures 6 and 8 that polymer additives in repair material C cause a substantial increase in the longitudinal strain capacity. It is also evident that the use of high strength repair material A will increases the possibility of a brittle and sudden failure.

Practical Implications of Results

It is well established that it is economical to use aggregates in concrete mixes, which also lead to a technically superior material due to the dimensional stability, ductility and stiffness

TABLE 3

Instantaneous Elastic Strains on Loading and Creep Strains at 90 Days (Microstrain) and Cube Strength Prior to Loading

Repair Materials ⇨		A	B	C	Concrete
30% stress/strength	Cube strength (N / mm^2)	60	33	40	38
	Instantaneous elastic strain	488	442	553	454
	creep strain	1217	1212	1871	1446
45% stress/strength	Cube strength (N / mm^2)	60	37	43	40
	Instantaneous elastic strain	704	749	893	866
	creep strain	2078	2161	2552	2148
55% stress/strength	Cube strength (N / mm^2)	63	36	38	35
	Instantaneous elastic strain	949	1129	1039	954
	creep strain	3129	2767	3137	2732

provided by aggregate to the cement paste matrix [17]. Similar benefits can be achieved by using fine and coarse aggregate size particles in repair mixes. Polymer additives in repair material show a great improvement in post-peak strain capacity but at the same time they increase the long-term shrinkage and creep deformations. The long-term cracking at the repair/substrate interface and the load sharing by the repair patch is primarily controlled by the shrinkage and creep characteristics of the repair materials. While the load distribution controlled by the elastic modulus property of these materials. It is clear from the results of material C that total shrinkage strains are greatest for this material but the compressive strength, stiffness and strain capacity are similar to those of good quality concrete. This suggests that patched repaired with material C could lead to unacceptably high tensile strains at the interface with the substrate with the consequent danger of cracking and adhesion failure. The high creep strains of material C relative to concrete, on the other hand, would help in reducing the tensile strains at the interface. Also, the stress-longitudinal strain relationship in Figure 6 for material C shows much greater non linearity than other materials which results in very low stiffness of the material at higher stress. This implies that the load sharing capacity of this material with the substrate will be very low and although material displays high strain capacity at failure, this strain capacity would not contribute effectively to stress redistribution in the patch repair. The material is, therefore, more suitable for cosmetic repair application instead of repair which provides effective structural interaction. Repair material B has similar stiffness as concrete but the strain capacity at a maximum load is very low (less than 1400 microstrain compared to 2200 microstrain) this again would result in unsatisfactory load sharing with the substrate and material prone to cracking. If the excessively high elastic modulus material A (Table 1) is used for repair on a normal grade concrete substrate, excessive redistribution of stress to the patch would result causing an effect of eccentricity in the load distribution. Therefore, a high strength and consequently high elastic modulus of the repair material A will increases the load sharing capacity of the repair patch, but it will also increase the possibility of cracking and brittle failure.

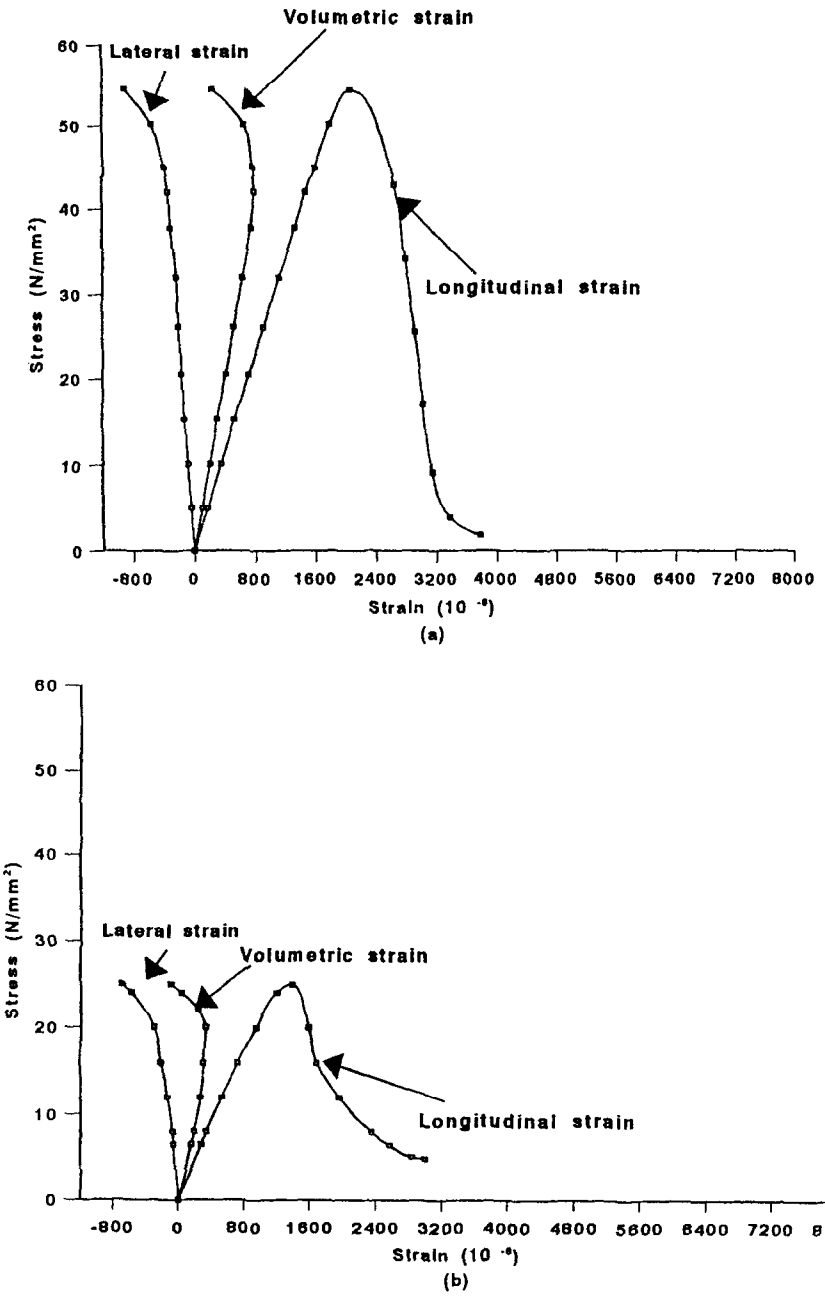

FIG. 6.
Stress-strain curves of (a) material A, (b) material B, (c) material C and (d) plain concrete.

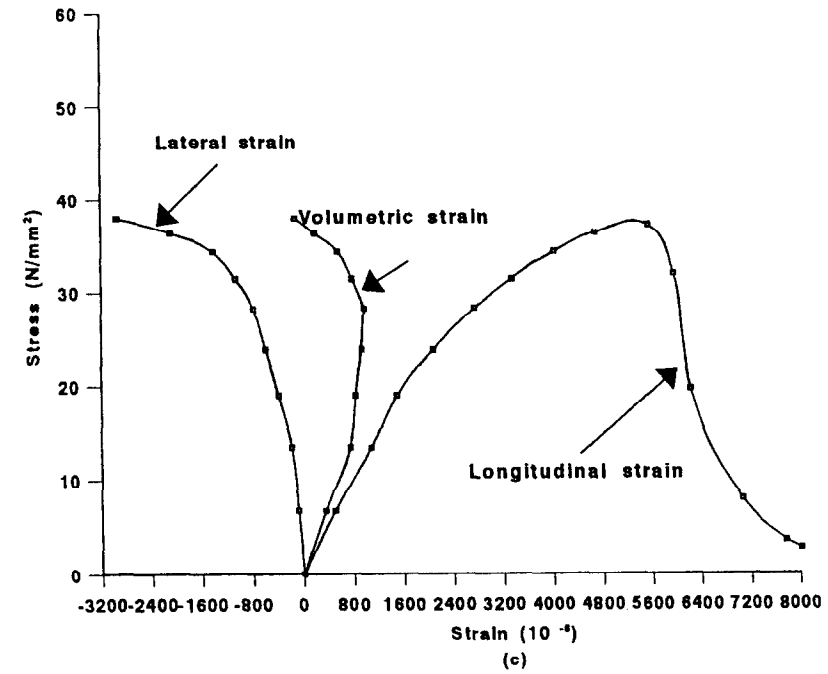

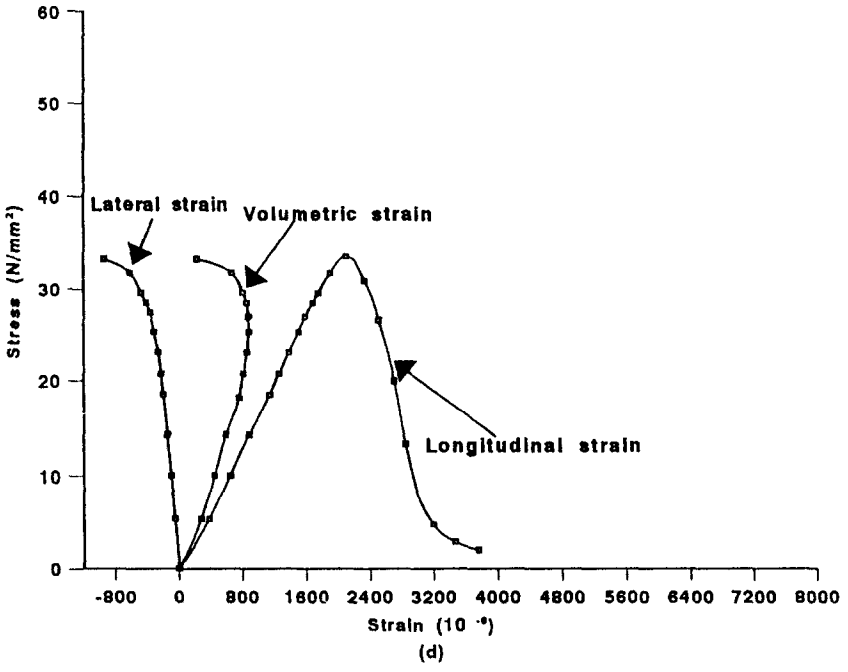

FIG. 6. *Continued*

TABLE 4

Stress-Strain Results for Repair Materials and Concrete Specimens

Materials⇨			A	B	C	Concrete
Cube Strength (N/mm^2)			63.7	33.0	44.05	41.0
Initiation Stress	Stress / strength ratio		0.47	0.39	0.28	0.55
	Strain (10^{-6})	longitudinal	486	520	499	885
		lateral	83	90	94	154
		volumetric	320	340	311	577
Critical Stress	Stress / strength ratio		0.83	0.80	0.78	0.80
	Strain (10^{-6})	longitudinal	1587	1417	2740	1270
		lateral	395	650	789	240
		volumetric	797	117	1162	790

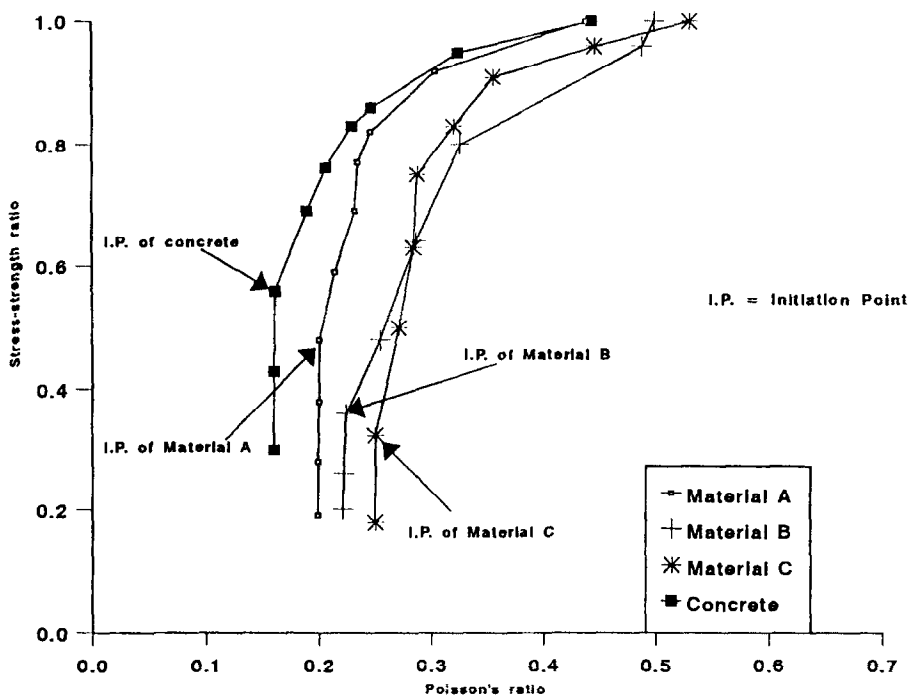

FIG. 7.
Relationship between stress-strength ratio and poisson's ratio.

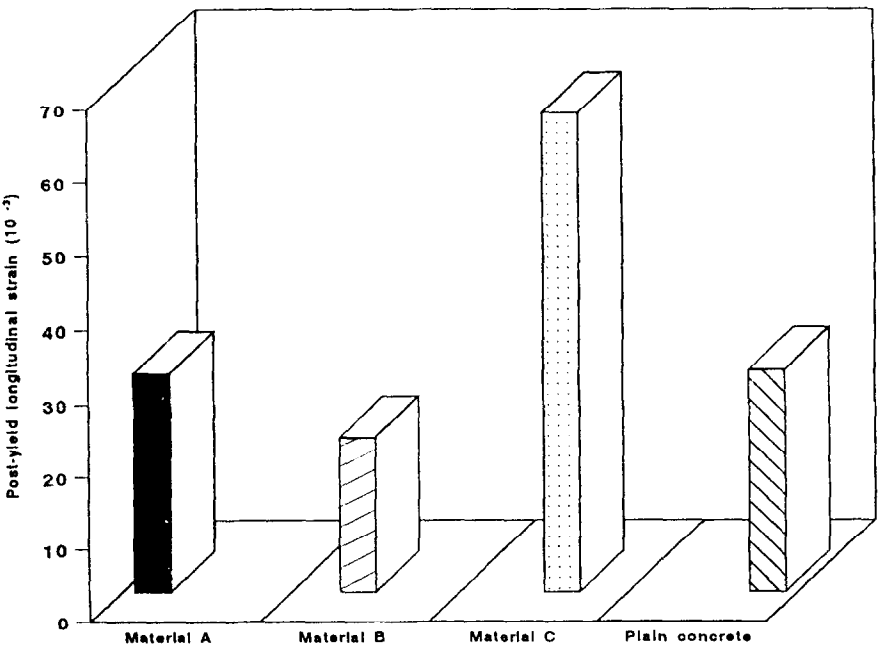

FIG. 8.
Longitudinal strain at a post-peak stress-strength ratio of 0.4.

Conclusions

The following conclusions are based on the experimental results reported in this paper on the repair material properties for effective structural application:

1. The highest values of strength and modulus of elasticity are associated with the cementitious repair material which contains aggregate particles and has a low water/powder ratio.
2. Total shrinkage strains are greatest for the polymer modified cementitious mortar despite the presence of some fibre additives. In all cases, most of the shrinkage occurs within the first three weeks and remains relatively stable beyond that age. Also, the relative humidity of exposure has a significant effect on the shrinkage deformation of repair materials compared to normal concrete.
3. Compressive creep strains are greatest for the mortar which contains styrene acrylic copolymer, compared to other materials.
4. The ultimate stress level (at maximum load) of repair materials varies significantly, the lowest ultimate stress being recorded for the porous mineral based material B. For example, average value of ultimate stress for materials A, C and control concrete were 62, 47 and 50 N/mm^2 respectively, while for material B it was 25 N/mm^2. The post-peak strain capacity of the material modified with a polymer admixture, material C, is markedly improved leading to a more pronounced falling branch of stress-strain curve whereas the test specimens of high strength repair material A fail in a brittle manner.

Acknowledgments

This paper presents some of the results of an EC supported **BRITE / EURAM** research project **BREU P3091** "Assessment of Performance and Optimal Strategies for Inspection and Maintenance of Concrete Structures Using Reliability Based Expert Systems".

References

1. Swiss Bank Corporation (Stockbrokers). Quarterly Building Bulletin, London, p. 5, 1989.
2. P.C. Hewlett, and S.A. Hurley, Design Life of Buildings, Thomas Telford, London, 179-196, 1985.
3. N.K. Emberson, and G.C. Mays, Proc. ICPIC '87: 5th International Congress on Polymers in concrete, Brighton, 235-242 1987.
4. D.R. Plum, The Structural Engineer, 68, (17), 337–345 (1990).
5. J.G.M. Wood et al., Proceedings of Structural Faults Repairs '89, Vol. 2, London,1989, pp 231-236.
6. N.K. Emberson, and G.C. Mays, Mag. of Concrete Research, 42, 152, 147-160, 1990.
7. BS 12, Standard Specification for Portland Cements, British Standard Institution, London
8. BS 1881, Part 116, British Standard Institution, London, 1983.
9. BS 1881, Part 118, British Standard Institution, London, 1983.
10. BS 1881, Part 121, British Standard Institution, London, 1983.
11. J.M. Illston, and C.D. Pomeroy, Concrete, pp 24-25 1975.
12. J.M. Smith, and L.E. Young, ACI Journal Proceedings, 52, (3), 349–359 (1995).
13. S.P. Shah, A.E. Naaman, and J. Moreno, The International Journal of Cement Composites and Light Weight Concrete. 5, (1), 15–25 (1983).
14. W.C. Halabi, PhD thesis, University of Aberdeen, UK,1991.
15. S.P. Shah, and S. Chandra, Journal of ACI. 65, 770–781 (1968).
16. T.V. Zaitsev, Cement and Concrete Research, 1, (1), 123–137 (1971).
17. A.M. Neville, Properties of Concrete. ELBS, 3rd Edition, pp. 118-202, 1983.